APL Materials

Liquid electromigration in gallium-based biphasic thin films

Cite as: APL Mater. **7**, 031504 (2019); https://doi.org/10.1063/1.5059380
Submitted: 20 September 2018 . Accepted: 23 December 2018 . Published Online: 07 February 2019

Hadrien O. Michaud, and Stéphanie P. Lacour

COLLECTIONS

Paper published as part of the special topic on Advances in Flexible and Soft Electronics

View Online Export Citation CrossMark

ARTICLES YOU MAY BE INTERESTED IN

Stretchable conductive nanocomposite based on alginate hydrogel and silver nanowires for wearable electronics
APL Materials **7**, 031502 (2019); https://doi.org/10.1063/1.5063657

Invited Article: Emerging soft bioelectronics for cardiac health diagnosis and treatment
APL Materials **7**, 031301 (2019); https://doi.org/10.1063/1.5060270

Bilayer nanocarbon heterojunction for full-solution processed flexible all-carbon visible photodetector
APL Materials **7**, 031501 (2019); https://doi.org/10.1063/1.5054774

© 2019 Author(s).

Liquid electromigration in gallium-based biphasic thin films

Cite as: APL Mater. 7, 031504 (2019); doi: 10.1063/1.5059380
Submitted: 20 September 2018 • Accepted: 23 December 2018 •
Published Online: 7 February 2019

View Online Export Citation CrossMark

Hadrien O. Michaud and Stéphanie P. Lacour[a)]

AFFILIATIONS

Bertarelli Foundation Chair in Neuroprosthetic Technology, Laboratory for Soft Bioelectronic Interfaces, Institute of Microengineering, Institute of Bioengineering, Center for Neuroprosthetics, Ecole Polytechnique Fédérale de Lausanne (EPFL), 1202 Geneva, Switzerland

[a)]Author to whom correspondence should be addressed: stephanie.lacour@epfl.ch

ABSTRACT

Liquid metals have recently gained interest as a material of choice for soft and stretchable electronic circuits, thanks to their virtually infinite mechanical failure strain and high electrical conductivity. Gallium-based thin films are obtained by depositing gallium in the vapor phase to form a class of liquid metal conductors. The films, with an average thickness below 1 μm, withstand mechanical strain in excess of 400%. However, modes of failure other than mechanical ones have not yet been thoroughly investigated. In particular, electromigration, a well-known cause of failure in solid thin film traces for integrated circuits, also occurs in bulk liquid metals. In this work, microscopic observation of the thin conductive traces reveals that gallium is displaced from the anode terminal toward the cathode terminal after direct current stressing. This results in a catastrophic increase in the trace resistance and electrical failure. The mean time to failure decreases with increasing current density, following Black's equation, an empirical mathematical model originally developed to describe failure in solid metal thin-film tracks due to electromigration. We show that using alternating current, e.g., symmetric square wave, rather than direct current can extend the lifetime of the thin liquid metal film conductor by several orders of magnitude. These results may help stretchable circuit designers who select liquid metal thin-film conductors as the stretchable interconnect technology to predict devices' lifetime and implement mitigation strategies at the system level or at the material level.

© 2019 *Author(s). All article content, except where otherwise noted, is licensed under a Creative Commons Attribution (CC BY) license (http://creativecommons.org/licenses/by/4.0/).* https://doi.org/10.1063/1.5059380

The mechanical stiffness of conventional electronic materials and the form factor of electronic components and circuits slow down their deployment in applications where conformability and motion are essential, such as soft robotics, wearable, on-skin, monitoring, and implantable electronic interfaces.[1-3] Stretchable electronics is a field of research that consists in overcoming these limitations by engineering and integrating alternative approaches based on soft, highly deformable materials.[4] Stretchable conductors are an essential component for the realization of such conformal circuits. They enable distribution of electrical power and transmission of analog or digital signals between the components of the circuits. Among the solutions available to form stretchable conductors, liquid metals are particularly interesting because they can withstand repeated and virtually infinite strains while maintaining a high electrical conductivity.[5] Gallium based alloys such as gallium indium eutectic (EGaIn) are liquid near room temperature (29.7 °C for pure Ga and 15.7 °C for EGaIn) and do not display known toxic reactions.[6] However, processing and patterning these metallic alloys with standard liquid printing techniques, e.g., ink-jet or screen printing, are difficult tasks because of the high surface tension of the liquid metals and the formation of a few nanometer thick solid oxide skin at their surface upon contact with oxygen.[7] It is particularly challenging to pattern uniform micron-scale structures of liquid metal films over large (>10 cm^2) surface areas.

To overcome these manufacturing limitations, our group introduced a physical vapor deposition (PVD) process to form gallium-based films.[8] The films are obtained by evaporating gallium on a silicone rubber substrate, preliminarily coated

© Author(s) 2019

with a thin (60 nm) layer of gold. A film composition of 92.8 at.% Ga was experimentally determined as an optimal trade-off between the quantity of evaporated gallium and the electromechanical performance of the films: doubling the quantity of deposited gallium to reach 96.2 at.% Ga only resulted in a minimal decrease in resistivity and sensitivity to mechanical strain.[8] At 92.8 at.% Ga, the biphasic films are composed of a solid $AuGa_2$ phase and a liquid Ga phase intertwined in a sub-micrometer layer, and large microscopic Ga bulges randomly scattered at the surface of the film. As detailed in previous work,[8] Ga remains liquid in the film even at room temperature–below 29.7 °C, the melting point of Ga–due to a strong supercooling effect. This class of conductors demonstrates exceptional resistance to repeated mechanical stress (e.g., one million cycles to 50% uniaxial strain) while maintaining finite electrical resistance under strains exceeding 400%. Using lift-off photolithography, Ga-based conductive traces with line widths down to 10 μm can be patterned at the wafer scale and offer design freedom to prepare a range of wearable sensors and interconnect layouts for power-demanding devices like LEDs.[8,9] In this later case, electrical stability of the interconnects upon prolonged stressing (in addition to mechanical robustness) defines the lifetime of the circuit.

In this study, we report on an electrical failure mode in thin liquid metal-based conductors. Electromigration is a known deterioration process in thin film metallic tracks and has been extensively documented in the context of integrated circuits. In solid films, electromigration is defined by the net displacement of the metal ions in the conductor under the action of the flux of electrons when the conductor carries electrical current.[10] If current stressing is sustained over time, it will ultimately result in physical discontinuity and failure of the metallic trace. The higher the current density in a trace, the more important the effect of electromigration is. Electromigration not only occurs in solid metals but has also been reported for bulk liquid metals.[11]

We observed the following sequences in evaporated biphasic Ga films. The thinnest portions of the evaporated Ga films on polydimethylsiloxane (PDMS) are typically of a few 100s nm thick, which results locally in high current density upon DC bias. Under direct current (DC) stressing, gallium is displaced from the anode terminal to the cathode terminal. The resulting electrical resistance of the traces dramatically increases until electrical failure and open circuit condition. The mean time to failure decreases with increased current density. Applying alternating current (AC) instead of DC current greatly enhances the lifetime of the conductors under current stressing. In this letter, we report on the occurrence of electromigration in thin Ga-based biphasic films, model its dynamics, and investigate possible mitigation strategies.

Conductive traces were prepared following the process flow described in Ref. 8. Float glass wafers were coated with a 120 μm layer of poly(dimethylsiloxane) (PDMS, Sylgard 184, Dow Corning) spin-coated at 500 rpm and cured in an oven at 80 °C for 2 h. Polyethylene terephthalate (PET) stencil masks were cut and laminated on the PDMS. 60 nm of gold was then sputtered at room temperature (AC 450, Alliance Concept), and gallium was thermally evaporated (E300, Alliance Concept) to reach 92.8 at.% Ga in the film; this composition was selected since a further increase in the gallium content in the films only resulted in minimal improvements in conductivity and electromechanical performance.[8] Finally, conductive traces terminated by connection pads were patterned by peeling off the PET stencil masks.

The films were composed of a sub-micrometer thin flat base onto which liquid gallium bulges were randomly distributed [Figs. 1(a)–1(c)]. To determine the overall topography of the films, we used a confocal laser microscope (LEXT OLS4100, Olympus, pixel size 625 × 625 nm^2), which has a maximum vertical accuracy of 200 nm and can image reflective samples with slopes up to 85°. The bulges could reach up to 100 μm in circumference and up to 20 μm in height for films with 92.8 at.% Ga. More than 80% of the film surface area remained under 1 μm, and more than 97% remained under 5 μm (see Fig. S1 in the supplementary material). To precisely determine the average thickness of the flat solid-liquid part of the film, we utilized a white light interferometer (ContourGT- K, Bruker, pixel size 1 × 1 μm^2) in the vertical scanning interferometry (VSI) mode. The white light interferometer had a vertical resolution limit of 3 nm but could not measure steep slopes on reflective materials. A feature recognition routine detailed in Fig. S2 in the supplementary material was used to identify the bulges at the surface of the film and compute the thickness and roughness of the flat film area.

The mean measured thickness of the flat portions of the film at the center of a wafer was 370 nm with a mean RMS roughness of 80 nm [Figs. 1(e)–1(g) and S3 in the supplementary material]. The mean measured thickness corresponded to the thickness of the $AuGa_2$ alloy measured from a single cross section scanning electron microscope (SEM) image, and the RMS roughness value was in agreement with atomic force microscope (AFM) measurements.[8] The measured thickness and topography can be used in finite element simulations to estimate the maximum current density in the films.[12]

Electromigration in solid metals refers to the displacement of the conductor's atoms under the action of an electrical current and has a crucial influence on the reliability of integrated circuits.[10] It results from the collisions between the free electrons and the atoms in the conductor's lattice. Following the "electron wind" direction, the metal atoms drift toward the anode, preferably through grain boundary vacancies in polycrystalline thin films.

Dutta and co-workers reported extensively on macroscopic electromigration in liquid metals and in particular in gallium.[11,13,14] The electromigration force $\vec{F}$ exerted on the metal ions is the resultant of two forces with opposite directions, the electrostatic force and the force exerted by the electron wind. The total force is

$$\vec{F} = (Z + Z_w)e\vec{E} = Z^* e\vec{E}$$

with Z being the ion valence, Z_w being the valence resulting from ion-electron wind coupling, and Z^* being the effective valence accounting for both the electrostatic force and the

© Author(s) 2019

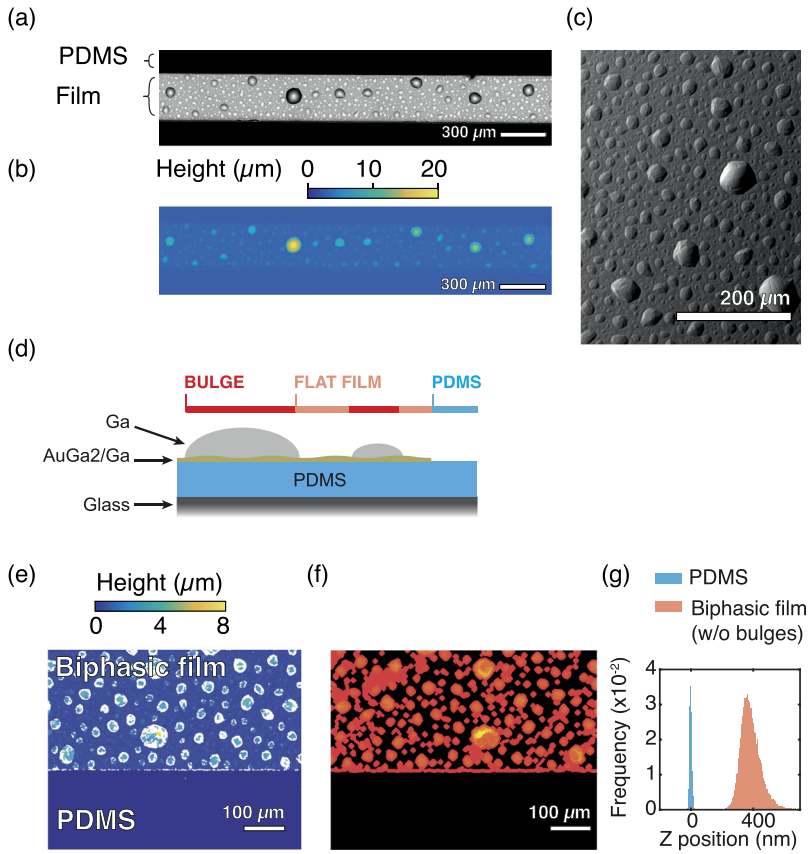

FIG. 1. Topography of the biphasic films with 92.8 at. % Ga. (a) Laser confocal microscope image. (b) Corresponding height profile. (c) SEM picture obtained with the secondary electron (SE) detector for topography contrast. (d) Schematic cross section highlighting the different areas composing the film and the subtrate: bulges, flat film, and PDMS. (e) Topographic images of three zones from white light interferometry measurements. The upper half of the images is the biphasic film, while the lower half is the PDMS substrate. White pixels indicate that no data could be collected due to large slopes. (f) Bulges identified using the image analysis routine for bulge detection detailed in Fig. S2 in the supplementary material and missing data are identified in red. (g) Height histograms of PDMS (blue) and biphasic flat film without bulges (orange).

electron wind force, $\vec{E}$ being the electric field, and e being the elementary charge.[10] In solid conductors, the wind force dominates: $Z^* < 0$, and electromigration occurs in the direction opposite to the electrical field (from the cathode to anode). In some liquid conductors, the electrostatic force dominates: $Z^* > 0$, and electromigration occurs in the direction of the electrical field (from the anode to cathode).[11,13]

In microelectronics reliability studies, the failure time of a thin film metallic interconnect is typically defined as the time required to reach a fixed fraction increase in resistance from the initial resistance of the interconnect.[15–17] The mean time to failure $t_{fail,50}$ is empirically described by the generalized Black's equation,[18,19]

$$t_{fail,50} = \frac{A}{j^n} e^{\frac{E_a}{kT}},$$

where A is a constant, E_a is the activation energy for failure, k is the Boltzmann constant, T is the temperature, and n is a fitting parameter. n is typically between 1.5 and 7 for solid thin film metallization technologies.[19]

The effects of electromigration in metallization technologies and the agreement with Black's equation are typically determined by performing stress tests at different current intensities. Figure 2 shows the setup we used for the current stressing tests in the biphasic thin films. The traces were 1 mm wide and 15 mm long. Based on previous work, we selected the trace's width to maintain the increase in temperature from room temperature due to Joule heating well below values that could have damaged the PDMS substrate ($\Delta T < 12\,^{\circ}C$ for 30 mA flowing through a 1 mm-wide trace with 92.8 qt. % Ga).[8] The wafers supporting the tested samples were placed in a probe station (MPS 150, Cascade Microtech). We probed the traces

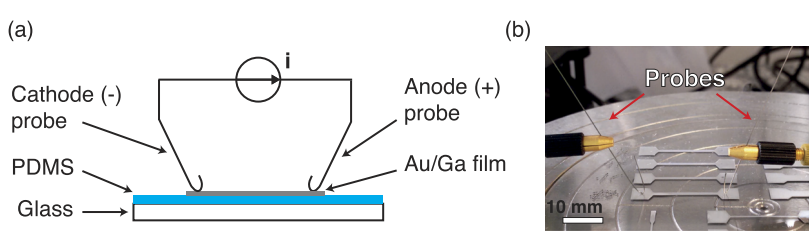

FIG. 2. Test setup for current stressing tests. (a) Schematic representation of the setup for current stressing. (b) Picture of the setup with structures under test.

© Author(s) 2019

using curved tungsten wires (99.9% purity, 0.25 mm diameter, Electron Microscopy Sciences) mounted on micrometric positioning probes (DPP210, Cascade Microtech). Tungsten was chosen as the contacting material since it is resistant to corrosion by gallium.[20] The mean interprobe distance was 18.0 ± 0.3 mm (mean ± S.D., n = 15). DC current was passed through the tracks, and the resistance was recorded using a source-meter (2400, Keithley).

The samples were observed with an optical microscope (Eclipse, Nikon) and a scanning electron microscope (Merlin, Zeiss) before and after applying the DC current. Energy dispersive spectroscopy (EDS) data were acquired in the SEM at a beam energy of 20 keV, using a 50 mm^2 silicon drift detector (X-Max, Oxford Instruments), and analyzed using the Aztec software from the same supplier.

We observed a drastic change in the film aspect in proximity to the tungsten probes [Figs. 3(a) and 3(b)]. Before failure and after probing, both anode and cathode contact areas had a metallic aspect. After failure, the anode area became darker, with metallic clusters randomly scattered. On the contrary, the cathode area retained its original metallic aspect. Liquid gallium bulges remained visible or even grew in size in the cathode area, whereas they disappeared in the anode area. We did not observe damage or micro-structural change in the central area of the traces.

EDS-SEM analysis after electrical failure revealed that in the anode area, gallium and gold were almost exclusively concentrated into the microscopic metallic clusters, while they were evenly distributed in the cathode area [Figs. 3(c) and 3(d)]. The metallic micro-clusters were composed of disjointed crystallites [inset Fig. 3(c)], which we identified as the $AuGa_2$ intermetallic alloy.[8,21] Interestingly, the observed $AuGa_2$ crystallites could reach sizes several orders of magnitudes larger than the initially deposited Au thickness (60 nm). It may come from the dissolution of smaller $AuGa_2$ particles and their re-aggregation into larger, more thermodynamically favorable crystallite, a process known as Ostwald ripening or coarsening.[22]

The resistance of the tracks increased dramatically over time under DC current stressing [Fig. 4(a)]. The initial mean

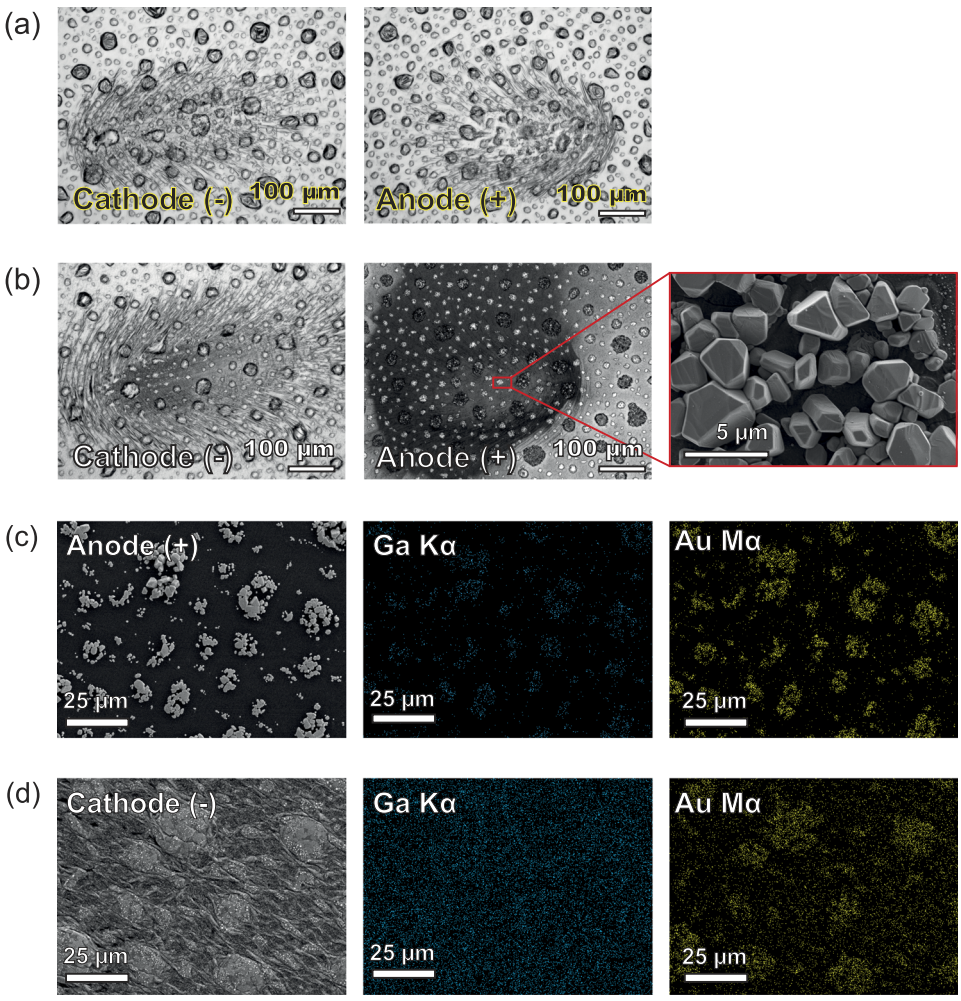

FIG. 3. Biphasic film before and after electrical failure. (a) Typical aspect of the cathode and anode areas observed with an optical microscope after probing and before electrical failure. (b) Typical aspect of the cathode and anode areas observed with an optical microscope after electrical failure. The inset shows crystallites observed with the SEM. (c) SEM image and corresponding EDS elemental map for the anode area. (d) SEM image and corresponding EDS elemental map for the cathode area. The EDS spectra corresponding to the maps are displayed in Fig. S4 in the supplementary material.

© Author(s) 2019

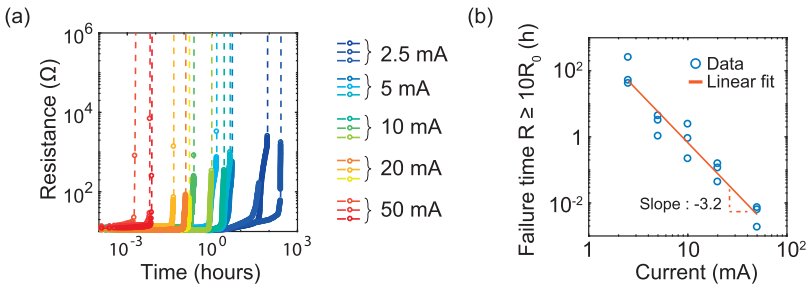

FIG. 4. Resistance of tests tracks as a function of time and failure time as a function of DC current. (a) Resistance as a function of time for 15 test tracks under DC current stressing (log-log plot). (b) Failure time, defined as the time required to reach 10 times the initial resistance R_0, as a function of current (log-log pot). R^2 = 0.93 for the linear fit.

resistance R_0 of the samples was 11.6 ± 0.9 Ω (mean ± s.d., n = 15 samples). We defined the failure time t_{fail} as the time when the resistance of the sample reached $10R_0$. The failure time followed an inverse power law as a function of the applied current $t_{fail} \propto I^{-m}$ with m = 3.2 [log-log plot Fig. 4(b)]. From measurements of the contact surface between the probes and the films [$A_{contact}$ =(49 ± 3) × 10 μm^2, mean ± s.d., n = 3], we estimated that the current density j at the contact area was between 5 A/cm^2 for I = 2.5 mA and 100 A/cm^2 for I = 50 mA.

In brief, we observed two phenomena:

- gallium was depleted near the anode terminal area and accumulated near the cathode terminal.
- the failure time of the tracks followed an inverse power law function of the DC current applied in the tracks.

Both observations are consistent with previous work on electromigration in liquid metal[11,13] and strongly support liquid electromigration as the predominant failure mode during DC current stressing tests. It also suggests that Black's equation can be used to link the current density and the speed of the induced electrical breakdown. The value of the current exponent (m = 3.2) is within the reported interval for current exponents in solid thin film metallization (1.5–7).[19] To our knowledge, no value was previously reported for liquid conductors.

If significant current must pass through thin film interconnects that may fail because of electromigration, mitigation strategies such as AC current powering can be considered to extend devices' lifetime.[23] To verify the applicability of this method with biphasic thin films, we contacted sample tracks (15 mm in length, 0.3 mm in width) terminated by contact pads using tungsten clamps. Current stressing was applied using either a sourcemeter (2400, Keithley) for DC current or a function generator (33220 A, Agilent) for AC current. The AC current was passed by applying a voltage square wave (±0.5 V) with a frequency of 500 Hz, corresponding to 20 mA forward or reverse current for the initial sample resistance of 25 Ω. The resistance of the tracks was monitored using the sourcemeter.

The time to failure of the biphasic thin film interconnects was extended by three orders of magnitude when using AC instead of DC current supply for the same current magnitude and trace geometry (Fig. 5). Interestingly, one terminal of the trace that failed under AC current maintained a metallic aspect with gallium accumulation, while the other darkened (Fig. S5 in the supplementary material). As for samples that failed under DC current, we did not observe damage or micro-structural changes in the central area of the trace. It indicates a net gallium transport toward one of the terminals. It may happen because of a small parasitic DC offset or because the mass flow between one half-cycle and the next is not exactly mirrored.[24] As a result of physical changes in the trace (e.g., formation, growth, or nucleation of voids or local metal accumulation) from the very onset of current stressing, the reverse migration during one half-cycle never totally compensates the defects created during the previous half-cycle, resulting in irreversible and asymmetrical mass transport.

We characterized the electrical reliability of stretchable gallium-based biphasic films exposed to prolonged DC and AC current stressing. The films were locally thin (<400 nm), resulting in high current densities locally when large currents flow through the biphasic film tracks. We highlighted the effect of liquid electromigration in interconnects made from the films: they irreversibly failed electrically due to the displacement of gallium atoms away from the anode terminal and toward the cathode terminal of the traces. The relationship between the failure time and the applied current density was well described by the empirical Black's equation. This model may be useful to predict a device's lifetime, especially when connecting components requiring currents in the mA range

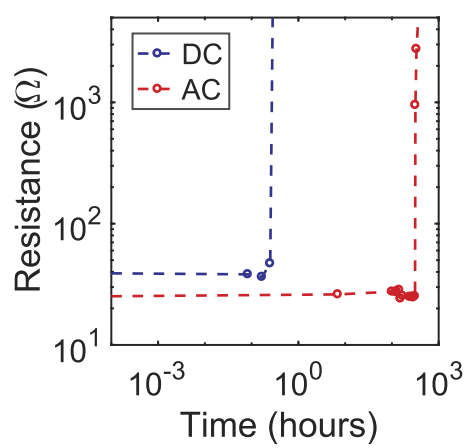

FIG. 5. Resistance of samples as a function of time for an applied DC current of 20 mA (blue) or an applied square wave AC voltage of ±0.5 V, corresponding to ±20 mA for the initial sample resistance of 25 Ω (red). Tested samples were tracks of 0.3 × 15 mm^2 with 92.8 at. % Ga contacted with tungsten clamps.

© Author(s) 2019

with small packages and pad sizes. We also verified that, as for solid thin film traces, applying bidirectional AC current stress instead of DC current stress resulted in extending the lifetime of the metallic traces by several orders of magnitude. As the use of DC or pulsed DC current is mandatory for some applications including light emitting diode (LED) powering, methods to increase the films' thickness and uniformity should also be investigated to reduce current densities in the interconnects and thus lengthen future devices' operational lifetime.[12] Other mitigation strategies could implement solid/liquid composite structures where the liquid phase is confined to generate a mechanical pressure that can locally counterbalance the electromigration force.[25,26]

See supplementary material for (1) cumulative density plot of biphasic film and bulges' height, (2) image processing routine for bulges' detection, (3) additional topography measurement to determine thin film thickness, (4) EDS spectrum corresponding to elemental maps in Fig. 4, and (5) optical microscope images of the biphasic films' surface after failure under AC current stressing.

We would like to thank Dr. Claudia Baumgartner from the University of Lausanne, and Blaise Rubinstein and Jakob Mallmann from Olympus who organized the measurement session with the confocal laser microscope. We acknowledge financial support from the Fondation Bertarelli and nano-tera.ch (No. 20NA_143070 WiseSkin).

REFERENCES

[1] H. Jin, Y. S. Abu-Raya, and H. Haick, "Advanced materials for health monitoring with skin-based wearable devices," Adv. Healthcare Mater. **6**(11), 1700024 (2017).

[2] S. P. Lacour, G. Courtine, and J. Guck, "Materials and technologies for soft implantable neuroprostheses," Nat. Rev. Mater. **1**, 16063 (2016).

[3] S. Coyle, C. Majidi, P. LeDuc, and K. J. Hsia, "Bio-inspired soft robotics: Material selection, actuation, and design," Extreme Mech. Lett. **22**, 51–59 (2018).

[4] T. Someya, Z. Bao, and G. G. Malliaras, "The rise of plastic bioelectronics," Nature **540**, 379–385 (2016).

[5] M. D. Dickey, "Stretchable and soft electronics using liquid metals," Adv. Mater. **29**(27), 1606425 (2017).

[6] M. D. Dickey, in *Stretchable Bioelectronics for Medical Devices and Systems*, edited by J. A. Rogers, R. Ghaffari, and D.-H. Kim (Springer International Publishing, 2016), pp. 3–30.

[7] I. D. Joshipura, H. R. Ayers, C. Majidi, and M. D. Dickey, "Methods to pattern liquid metals," J. Mater. Chem. C **3**, 3834–3841 (2015).

[8] A. Hirsch, H. O. Michaud, A. P. Gerratt, S. de Mulatier, and S. P. Lacour, "Intrinsically stretchable biphasic (solid–liquid) thin metal films," Adv. Mater. **28**, 4507–4512 (2016).

[9] H. O. Michaud, L. Dejace, S. de Mulatier, and S. P. Lacour, "Design and functional evaluation of an epidermal strain sensing system for hand tracking," in *2016 IEEE/RSJ International Conference on Intelligent Robots and Systems (IROS)* (IEEE, 2016), pp. 3186–3191.

[10] M. L. Dreyer and P. S. Ho, in *Handbook of Multilevel Metallization for Integrated Circuits*, edited by S. R. Wilson and C. J. Tracy (Noyes Publications, 1993).

[11] I. Dutta and P. Kumar, "Electric current induced liquid metal flow: Application to coating of micropatterned structures," Appl. Phys. Lett. **94**, 184104 (2009).

[12] A. Hirsch and S. P. Lacour, "A method to form smooth films of liquid metal supported by elastomeric substrate," Adv. Sci. **5**(10), 1800256 (2018).

[13] P. Kumar, J. Howarth, and I. Dutta, "Electric current induced flow of liquid metals: Mechanism and substrate-surface effects," J. Appl. Phys. **115**, 044915 (2014).

[14] S. Talukder, P. Kumar, and R. Pratap, "Electric current-induced mass flow in very thin infinite metallic films," IEEE Trans. Electron Devices **60**, 2877–2883 (2013).

[15] V. K. Andleigh, V. T. Srikar, Y. J. Park, and C. V. Thompson, "Mechanism maps for electromigration-induced failure of metal and alloy interconnects," J. Appl. Phys. **86**, 6737–6745 (1999).

[16] B. Li, J. Gill, C. J. Christiansen, T. D. Sullivan, and P. S. McLaughlin, "Impact of via-line contact on CU interconnect electromigration performance," in *2005 IEEE International Reliability Physics Symposium, 2005. Proceedings 43rd Annual* (IEEE, 2005), pp. 24–30.

[17] C. K. Hu, L. Gignac, and R. Rosenberg, "Electromigration of Cu/low dielectric constant interconnects," Microelectron. Reliab. **46**, 213–231 (2006).

[18] J. R. Black, "Electromigration—a brief survey and some recent results," IEEE Trans. Electron Devices **16**, 338–347 (1969).

[19] D. Young and A. Christou, "Failure mechanism models for electromigration," IEEE Trans. Reliab. **43**, 186–192 (1994).

[20] E. C. Miller, in *Liquid-Metals Handbook*, edited by R. N. Lyon (US Government Printing Office, 1952), pp. 144–183.

[21] R. P. Elliott and F. A. Shunk, "The Au-Ga (Gold-Gallium) system," Bull. Alloy Phase Diagrams **2**, 356–358 (1981).

[22] L. Ratke and P. W. Voorhees, *Growth and Coarsening: Ostwald Ripening in Material Processing* (Springer Science and Business Media, 2013).

[23] B. K. Liew, N. W. Cheung, and C. Hu, "Projecting interconnect electromigration lifetime for arbitrary current waveforms," IEEE Trans. Electron Devices **37**, 1343–1351 (1990).

[24] J. Tao, N. W. Cheung, and C. Hu, "An electromigration failure model for interconnects under pulsed and bidirectional current stressing," IEEE Trans. Electron Devices **41**, 539–545 (1994).

[25] I. A. Blech and C. Herring, "Stress generation by electromigration," Appl. Phys. Lett. **29**, 131–133 (1976).

[26] J. R. Lloyd, "Electromigration in integrated circuit conductors," J. Phys. D: Appl. Phys. **32**, R109–R118 (1999).

© Author(s) 2019